

P333

## Elastic Near-surface Attenuation Estimation for an Oman Seismic Data Set

N. El Yadari\* (Fugro Seismic Imaging Ltd) & W.A. Mulder (Shell International E&P BV)

### SUMMARY

---

In many onshore exploration areas, the near surface causes a dramatic deterioration of the quality of seismic data. In principle, full waveform inversion followed by redatuming should clean up the data. Full waveform tomography requires an accurate starting model. We assume that a kinematic method can provide velocities and densities and focus on the determination of an elastic near-surface attenuation model. Earlier, we proposed a method that estimates the near-surface attenuation properties using visco-acoustic finite-difference modelling. Here, we extend the method to the visco-elastic, horizontally layered case using the reflectivity method. We consider the effect of P- and S-waves as well as the influence of deeper layers on the attenuation estimate. Application to synthetic and field data demonstrates the effectiveness of the method.

## Introduction

El Yadari et al. [1] developed an algorithm that uses the complete seismogram to estimate the near-surface attenuation properties. This algorithm was based on visco-acoustic wave propagation modelling. Given velocities and densities in a layered medium, we compared the energy decay along traveltimes curves in the modelled and observed seismic data for a range of attenuation parameters. The best match provided an estimate of the attenuation. A sensitivity study indicated that the picked reflected and refracted traveltimes and the near-surface model from refraction statics provided sufficient robustness against depth and velocity perturbations smaller than 10%. We included some of the complexity involved in the near surface. We incorporated elevation corrections in the reflection and refraction traveltimes used for picking amplitudes. The results showed a slightly enhanced resolution of the error image obtained with elevation corrections. The effect of geometrical spreading and the source wavelet were taken into account. The wavelet should be carefully estimated. Finally, we extended the technique to multiple layers. We applied the method to synthetic and to field data. In this paper, we extend the method to the visco-elastic case, using Kennett's reflectivity code. We first outline the method. We generalize the error criterion that compares the energy of modelled and observed seismograms along traveltimes curves from the acoustic to the elastic case. We then apply the method to synthetic data as well as field data from Oman to study the effect of P- and S-waves on the error as well as the influence of deeper layers on the attenuation estimates.

## Brief description of the method

The most common measure of attenuation is the dimensionless quality factor  $Q$ , the ratio of stored energy to dissipated energy. For details of the method and alternative attenuation descriptions, we refer the reader to an earlier article [1]. We consider a subsurface model that consists of horizontal strata with constant medium parameters in each layer. As before [1], we assume that a kinematic method can provide a horizontally layered model with density  $\rho_m$ , depth  $d_m$ , and velocities  $V_{Pm}$  and  $V_{Sm}$  for each layer labelled by  $m = 1$  to  $M$ . Hence, we assume that  $\rho$ ,  $d$ ,  $V_P$  and  $V_S$  (vectors with a length  $M$  equal to the number of layers) are known. We want to determine the attenuation parameters denoted by the vectors  $Q_P$  and  $Q_S$ . To achieve this, a set of  $N$  models characterized by  $Q_P^n$  and  $Q_S^n$ ,  $n = 1$  to  $N$ , is considered on a regular grid of values by starting from an initial guess. A forward modelling code simulates the full wavefield for each  $n^{\text{th}}$  subsurface model. The modelled seismogram resulting from each simulation is then compared to the observed one, leading to the desired attenuation model. The comparison step consists of picking the travel time for refracted and reflected P- or/and S-waves from each modelled and observed seismogram and selecting the corresponding energies. We determine the most likely attenuation model from the minimum value of an error criterion that measures the difference between the observed and the  $n^{\text{th}}$  synthetic seismograms as

$$E(Q_P^n, Q_S^n, W_t) = \frac{1}{M} \sum_{m=1}^M \alpha_m (E_m(Q_P^n, W_t) + E_m(Q_S^n, W_t)), \text{ and we impose } \sum_{m=1}^M \alpha_m = 1.$$

$\alpha_m$  is the weight assigned to the  $m^{\text{th}}$  layer.  $E_m(Q_P^n, W_t)$  and  $E_m(Q_S^n, W_t)$  are the errors corresponding to the  $m^{\text{th}}$  layer and given by the same expression  $E_m(Q^n, W_t)$  that we used earlier in the visco-acoustic case [1].  $E_m(Q^n, W_t)$  measures the difference between the energy inside a window, denoted by  $W_t$ , around the picked amplitudes from synthetic seismogram and observed seismogram. We denote these energies by  $\varepsilon^{\text{Synth}}$  and  $\varepsilon^{\text{Obs}}$ , respectively. Then,

$$E_m(Q^n, W_t) = \sum_{t=\text{Traces}} \left( \left| \log \left( \frac{\varepsilon^{\text{Obs}}(T_m^{\text{Ref}}(H_t))}{\varepsilon_n^{\text{Synth}}(T_m^{\text{Ref}}(H_t))} \right) \right| + \left| \log \left( \frac{\varepsilon^{\text{Obs}}(T_m^{\text{Ref}}(H_t))}{\varepsilon_n^{\text{Synth}}(T_m^{\text{Ref}}(H_t))} \right) \right| \right).$$

Note that  $T_m^{\text{Ref}}(H_t)$  and  $T_m^{\text{Ref}}(H_t)$  correspond, respectively, to the traveltimes of a ray reflected or refracted along the top surface of the  $m^{\text{th}}$  layer for a source-receiver distance denoted by  $H_t$ .

## Synthetic tests

We validated the method by performing a number of tests on synthetic data. We considered the effect of P- and S-waves on the error and examined the influence of deeper layers on the attenuation estimate. We used Kennett's public-domain reflectivity code [2], which operates in the slowness-frequency domain, to compute the seismic response of a horizontally layered medium to a vertical dipole source at the surface. We want to determine the attenuation for the near-surface model given in figure 1. For the modelling, we used frequencies between 10 and 54 Hz and the source wavelet displayed in figure 1 to transform the seismogram from the frequency domain to the time domain.

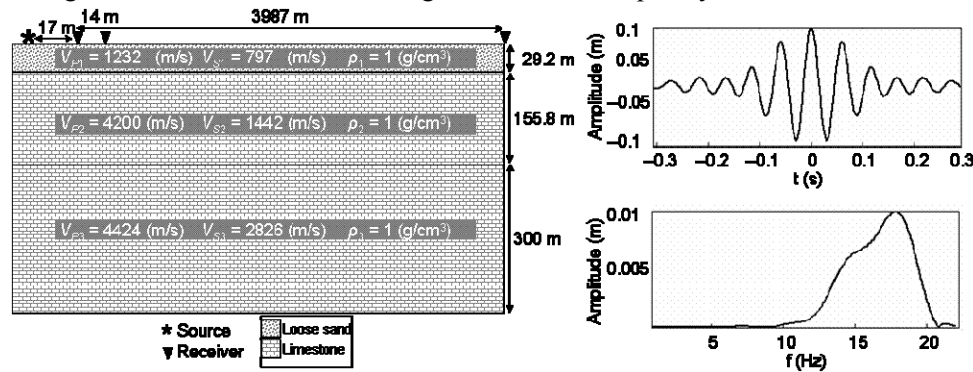


**Figure 1** Elastic subsurface model obtained from refractions statics. Wavelet estimated from the real data and its corresponding spectrum.

Our error criterion uses weight parameters  $\alpha_m$  and measures the energy in a strip around the picked traveltime curve of temporal width  $W_t$ . Consequently, we have to select suitable values for  $\alpha_m$  and  $W_t$ . In the visco-acoustic case [1], we obtained good results for  $\alpha_1 = \alpha_2 = 1/2$  and  $W_t = 0.1$  s. We justify our choice of alpha values by the intrinsic behaviour of the attenuation in upper and deeper layers:  $(Q_{P1}, Q_{S1})$  may affect  $(Q_{P2}, Q_{S2})$ , and  $(Q_{P3}, Q_{S3})$ . Also,  $(Q_{P1}, Q_{S1})$  and  $(Q_{P2}, Q_{S2})$  may affect  $(Q_{P3}, Q_{S3})$ , and so on. For this reason, we prefer to work with  $\alpha_1 = \alpha_2 = 1/2$ . Note, that  $\alpha_3$  is equal to 0 because the bottom of the fourth layer is absorbing and does not generate reflection or refraction events. Figure 2 presents the results of the sensitivity of the attenuation estimation to the use of P- and S-waves and to deeper layers. We computed two sets of seismograms while only varying the couples  $(Q_{P1}, Q_{S1})$  or  $(Q_{P2}, Q_{S2})$ . Ideally, the error surfaces should have a well-defined minimum at the correct value of the attenuation parameters, meaning that the error image should be bowl-shaped with a blue color at the correct minimum and rapidly and smoothly increasing values, from green to red, away from the minimum. The sharper the minimum, the better the resolution. In figure 2, the results show a

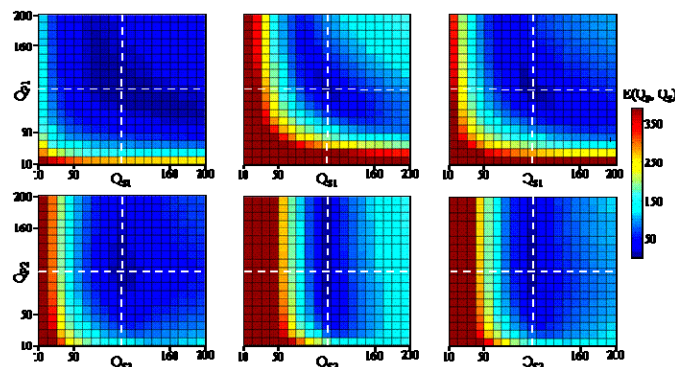


**Figure 2** Error surfaces obtained for the synthetic "observed" seismogram as a function of:  $Q_{P1}$  and  $Q_{S1}$  (1<sup>st</sup> row) or  $Q_{P2}$  and  $Q_{S2}$  (2<sup>nd</sup> row). We show separately, from the left to the right, error surfaces related to the energy picked for P-waves (1<sup>st</sup> column), S-waves (2<sup>nd</sup> column), or their combination (last column). The white dashed lines indicate the position of the minimum.

reasonably smooth behaviour of all error images. Also the correct parameter is always obtained at the minimum indicated by the dashed lines. However, we observe that the minimum becomes slightly less

well defined if we go from the first to the second layer (i.e. from the top to the bottom), implying that the resolution deteriorates if we go to the deeper layers. We may conclude that the attenuation estimation becomes more difficult if we go to the deeper layers. Next, we investigated the effect of P- and S-waves on the error. Figure 2 shows a considerably enhanced resolution of the image obtained with only S waves, especially for the top layer.

### Field data

We applied our method to a data set recorded in Oman. In [1], we demonstrated the need for an accurate estimate of the wavelet. We zero-phased a near-offset trace to determine the wavelet for the field data and only kept the part of its spectrum between 10 and 54 Hz (figure 1b). To construct an attenuation model, we proceed in a layer-stripping fashion. We first estimate the attenuation  $Q_{P1}$  and  $Q_{S1}$  in the top layer. Then, we try to find  $Q_{P2}$  and  $Q_{S2}$  and so on, up to  $Q_{P3}$  and  $Q_{S3}$ . To illustrate the effect of the window size  $W_t$  on the estimated energy  $\varepsilon$ , we calculated  $\varepsilon$  for four different values of  $W_t$  equal to 0.05 s, 0.1 s, 0.2 s, and 1 s. These values correspond to 1, 2, 4, and 20 wavelengths, respectively. Figure 3 shows independently for each type of wave the behaviour of the picked traveltimes for each layer as well as their sum and their corresponding energy decay curves for each value of  $W_t$ . We observe that for both type of waves the curves are quite similar for  $W_t = 0.1$  s and 0.2 s. These can be considered as reasonable values if we compare them to the associated wavelength. However, the energy decay curves for  $W_t = 1$  s are significantly different from the others. Also, in the case of P-waves, the energy decay curves related to  $W_t = 0.05$  s are slightly different from the ones obtained for  $W_t = 0.1$  s and 0.2 s. In the case of S waves, the wavelengths are shorter and the differences for various values of  $W_t$  are larger. The values of the energy, calculated for  $W_t = 0.1$  s, are then inserted into the error criterion to estimate how well the couples  $(Q_{P1}, Q_{S1})$  and  $(Q_{P2}, Q_{S2})$  explain the data. Note that the modelled energy values are calculated for each layer and are normalized by their maximum for that layer. For example, to estimate  $Q_{P1}$  and  $Q_{S1}$ , we constructed 400 synthetic seismograms for constant, large values of  $Q_{P2}, Q_{S2}, Q_{P3}, Q_{S3}$  equal to 1000, but for the  $Q_{P1}$  and  $Q_{S1}$  having values of 10, 20, ..., 200. This assumption is equivalent to considering only weak attenuation in the deeper layers. Then, each of the 400 modelled seismograms was compared with the field data. By analogy with the synthetic test, figure 4a shows the resulting error images as a function obtained with the energy picked for P- waves, S-waves, or their combination. The results exhibit a reasonably

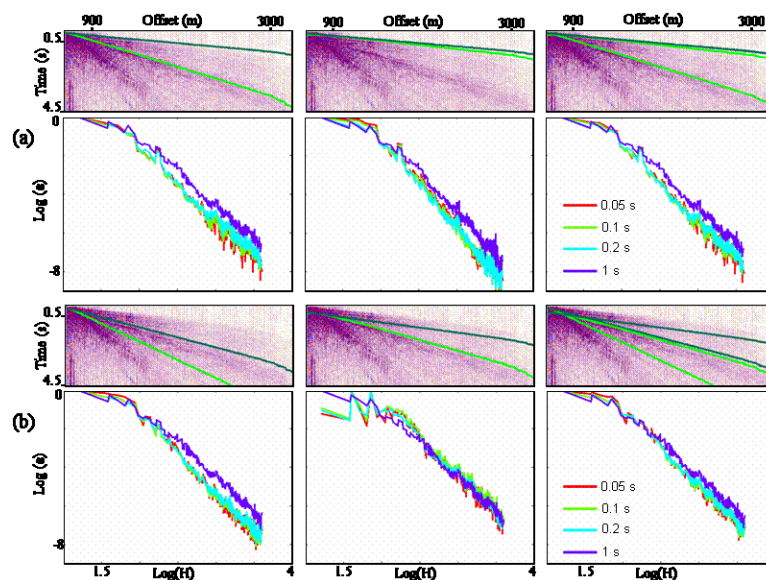


**Figure 3** Picked traveltimes curves and their corresponding energy decays for P-waves (a) and S-waves (b). For each case we show from the left to the right in the 1<sup>st</sup> row: refraction (dark green) and reflection (light green) traveltime curves picked on traces from the field data and calculated separately for the first layer (1<sup>st</sup> column) and the second layer (2<sup>nd</sup> column) as well as their total sum (last column). In the 2<sup>nd</sup> row, we display the energy decay for several values of the window size  $W_t$ .

smooth behaviour of the error surfaces corresponding to the top layer, unlike to the behaviour of the error surfaces related to the second layer. For example, the values of  $(Q_{P1}, Q_{S1})$  obtained at the minimum are equal to  $(10, 50)$ ,  $(10, 80)$ , and  $(10, 110)$ , from the left to the right. This means that  $Q_{S1}$  is not resolved and that the estimated values should follow the red dashed curve in figure 4a. This curve interpolates the values obtained at the minimum of  $Q_P$  for each fixed  $Q_S$ . If we require  $Q_P$  and  $Q_S$  to obey the empirical ratio between shear-wave and compressional-wave attenuation, namely  $Q_P = 2.25 Q_S$ , based on neglecting the dissipation in volume deformation, we can obtain a unique estimate for  $Q_P$  and  $Q_S$ . The straight line that represents this empirical ratio should intersect the interpolating curve for each error surface. Figure 4b shows the results of the estimated  $(Q_{P1}, Q_{S1})$  and  $(Q_{P2}, Q_{S2})$  obtained by this approach when considering P-waves, S-waves, or their combination. The estimated values of  $(Q_{P1}, Q_{S1})$  are equal to  $(34.2, 15.2)$ ,  $(21.4, 9.5)$ , and  $(26.3, 11.7)$ , respectively. We seem to have difficulty in estimating the values of  $(Q_{P2}, Q_{S2})$ , especially from the P-waves. This may be due to the fact that attenuation estimation becomes more difficult if we go to the deeper layers. Note that the estimated  $(Q_{P1}, Q_{S1})$  and  $(Q_{P2}, Q_{S2})$  agree with typical regional values inferred from shear-wave Q measurements given by [3].

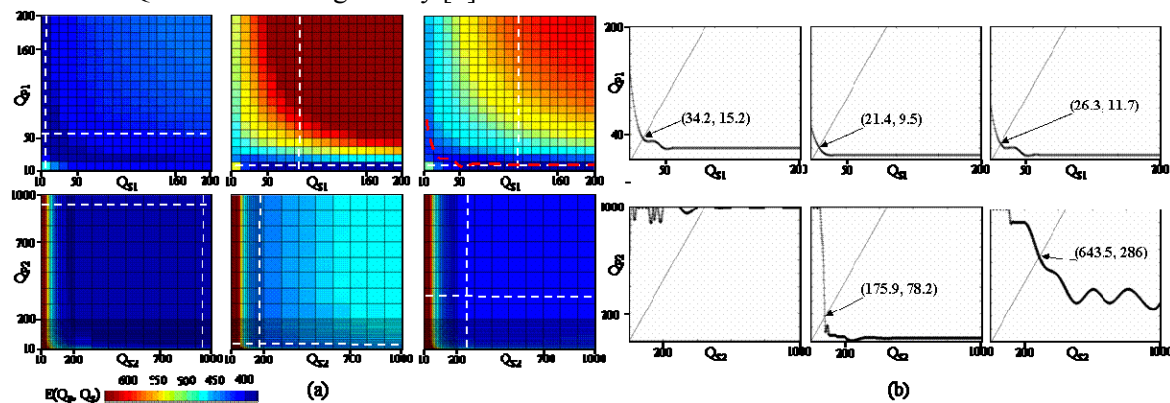


**Figure 4** (a) Error surfaces similar to those in figure 2, but for the field data. (b) Intersection between the line corresponding to the linear empirical relationship  $Q_P = 2.25 Q_S$  and the interpolated curve obtained by taking the minimum of  $Q_P$  at each  $Q_S$  in each of the error surfaces displayed in (a).

## Conclusions

We have presented a generalization of our attenuation estimation method from the visco-acoustic to the visco-elastic case. The method compares the energy decay between observed and modelled data along traveltime curves. We investigated the effect of P- and S-waves on the error as well as the influence of deeper layers on the attenuation estimate. The results showed that the attenuation estimation becomes more difficult if we go to the deeper layers, with a slightly enhanced resolution of the image obtained for only the S-waves, especially for the top layers. We applied the method to synthetic and to field data. The results for the latter agree with typical regional values. Further refinement of the method should involve forward modelling with topography and true source and the receiver elevations. This is especially important when the exploration target is a low-relief structure in an area with rough topography or complicated near surface.

## References

- [1] El Yadari, N., F. Ernst, and W. Mulder, 2008, Near-surface attenuation estimation using wave-propagation modelling, *Geophysics* 73, U27.
- [2] Kennett B.L.N. (1988). Systematic approximations to the seismic wave field, in *Seismological Algorithms*, ed. D.J. Doornbos, Academic Press, 237–259.
- [3] Mokhtar, T. A., R. B., Herrmann, and D. R., Russell, 1988, Seismic velocity and Q model for the shallow structure of the Arabian Shield from short-period Rayleigh waves: *Geophysics*, 53, 1379–1387.